



# Analysis of structural architecture in western Saudi Neom City area, northwestern Arabian Plate: Field investigation

Ali Y. Kahal<sup>\*</sup>, Essam Abd El-Motaal

Department of Geology and Geophysics, King Saud University, P.O. Box 2455, Riyadh 11451, Saudi Arabia

## ARTICLE INFO

### Keywords:

Dead Sea Transform  
Neom  
Transtension  
Negative flower structure  
Sinistral fault  
Arabian plate

## ABSTRACT

Saudi Neom City is being constructed as an urban mega-project in the northwestern part of the Arabian plate at the southeastern part of the NNE-oriented sinistral Dead Sea continental transform fault that links the NNW-oriented Red Sea Rift to the Zagros collision through the NE-oriented sinistral East Anatolian Fault. The present study aims to detect and analyze the different structural elements in the western Neom city. It also attempts to provide valuable data to help decision-makers for better achievement of such vital projects. From field investigation, the study area mainly comprises Neogene sedimentary sequence and exhibits a complex structural architecture represented by extensional- and wrench-style deformations. Different fault orientations (NNW–SSE striking extensional faults, WNW–ESE and ENE–WSW striking oblique-slip faults, and NNE–SSW and NNW–SSE striking strike-slip faults) dissect the western Neom area. Individual NNW-oriented Red Sea Rift-related extensional faults and fault blocks are antithetically tilted to the northeast. The sinistral movement onset along the Dead Sea Transform Fault postdates the Lower Miocene Burqan Formation deposition. Furthermore, the sinistral strike-slip regime of the western Neom area involves extensional structures, including normal faults, contractional structures (folds and reverse faults), and structures representing horizontal shear on near-vertical planes. NNW-oriented negative flower structures and forced folding occur along a synthetic NNW-oriented sinistral strike-slip fault set. Contractional structures are expressed by sets of NE-oriented left-handed en echelon-arranged folds in the Middle Miocene deposits. A proposed strain ellipse reveals these structures are associated with the NNE-oriented sinistral Dead Sea Transform Fault. The complexity of the structural architecture of the western Neom area can be attributed to its geologic setting under the influence of the Red Sea extensional rifting followed by the tectonic activity along the Dead Sea transform faulting. It is recommended that the structural attributes investigated, especially the geographic distribution of brittle structures (faults and fractures), be considered during the construction of Neom City.

## 1. Introduction

Neom City is geologically situated on the northwestern margin of the Arabian plate. The Red Sea rift bounds the southern side of Neom, and its western side is bordered by the Dead Sea Transform Fault (DSTF) (Fig. 1). The NNW-oriented Red Sea was initiated in the Oligo-Miocene as a continental rift splitting the Arabo-Nubian Shield into the Nubian Shield in Africa and the Arabian Shield in Asia. Consequently, the extending and subsiding Red Sea basin is flanked by high-relief shoulders reaching 2–3 km high in the southern Red Sea (Delaunay et al., 2023). As a result of erosion of these uplifting rift shoulders, the initial deposits of this basin consist mainly of siliciclastic sequences (Al Wajh and Burqan Formations) (Hughes and Filatoff 1995). As extension and

subsidence proceeded, the basin depositional environment became suitable for accumulating carbonates and evaporites (Maqna Group and Mansiyah Formation). From the Late Miocene to the Pleistocene, the deposits of the Red Sea basin are dominated by clastic assemblages (Ghawas, Lisan, and Ifal Formations). The structural architecture within the Red Sea rift is represented by numerous fault blocks bounded by NNW-SSE striking extensional faults and crossed by NE-SW transfer faults. Consequently, variable grabens, half-grabens, horsts, and step faults of different sizes have been formed along the Red Sea basin. Moreover, a rift-related neotectonic activity is expressed by the occurrence of Pleistocene-raised beaches along the Red Sea coast (Bosworth et al. 2017; Ribot et al. 2024).

The DSTF is a continental sinistral transform boundary, linking the

<sup>\*</sup> Corresponding author.

E-mail address: [akahal@ksu.edu.sa](mailto:akahal@ksu.edu.sa) (A.Y. Kahal).

<https://doi.org/10.1016/j.jksus.2024.103532>

Received 30 August 2024; Received in revised form 30 October 2024; Accepted 6 November 2024

Available online 8 November 2024

1018-3647/© 2024 The Authors. Published by Elsevier B.V. on behalf of King Saud University. This is an open access article under the CC BY-NC-ND license (<http://creativecommons.org/licenses/by-nc-nd/4.0/>).

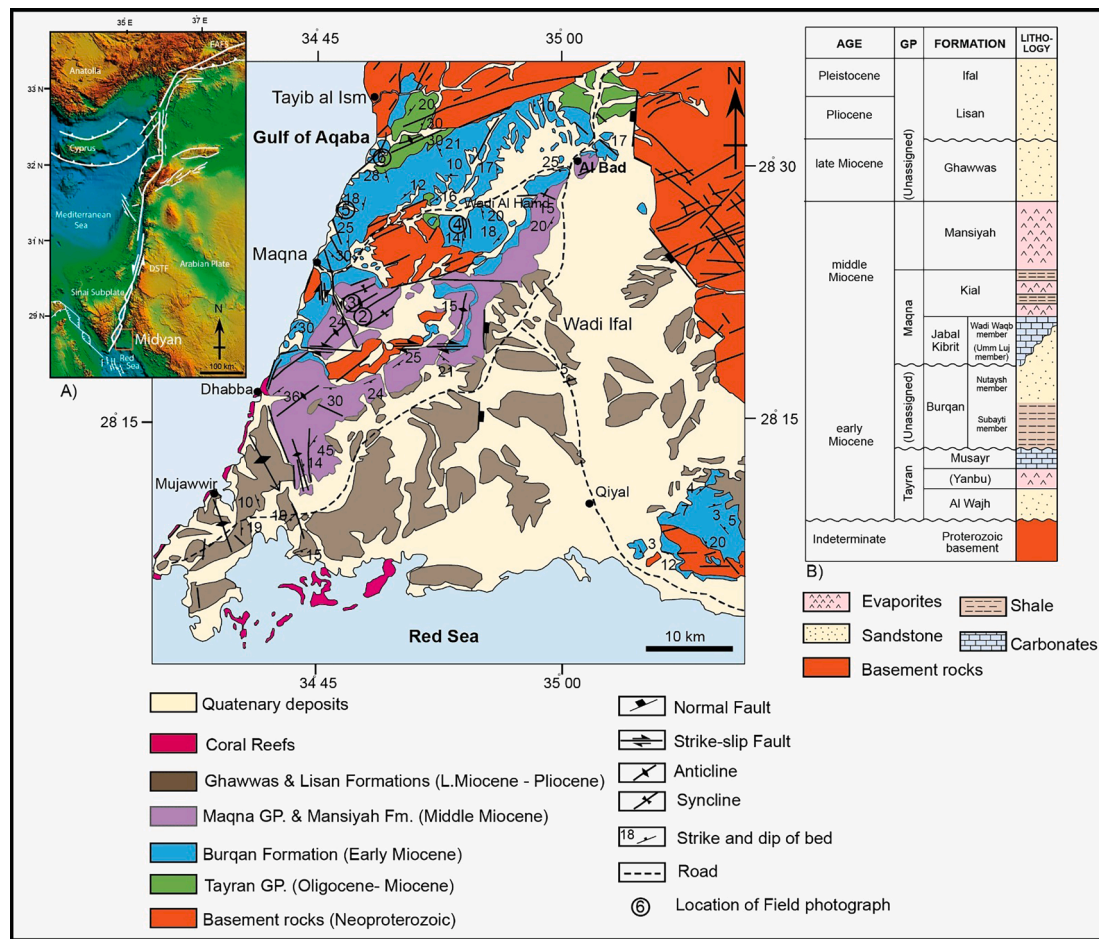


**Figure 1.** A. Geological map of the western Neom area in the northwestern Arabian plate (Clark, 1986; Hughes et al., 1999). The inset shows the tectonic framework of the Dead Sea Transform Fault (DSTF) (Daëron et al., 2004) and the location of the study area (red rectangle). EAFS is the East Anatolian Fault System. B. Columnar stratigraphic section of Neom area (Hughes et al., 1999).

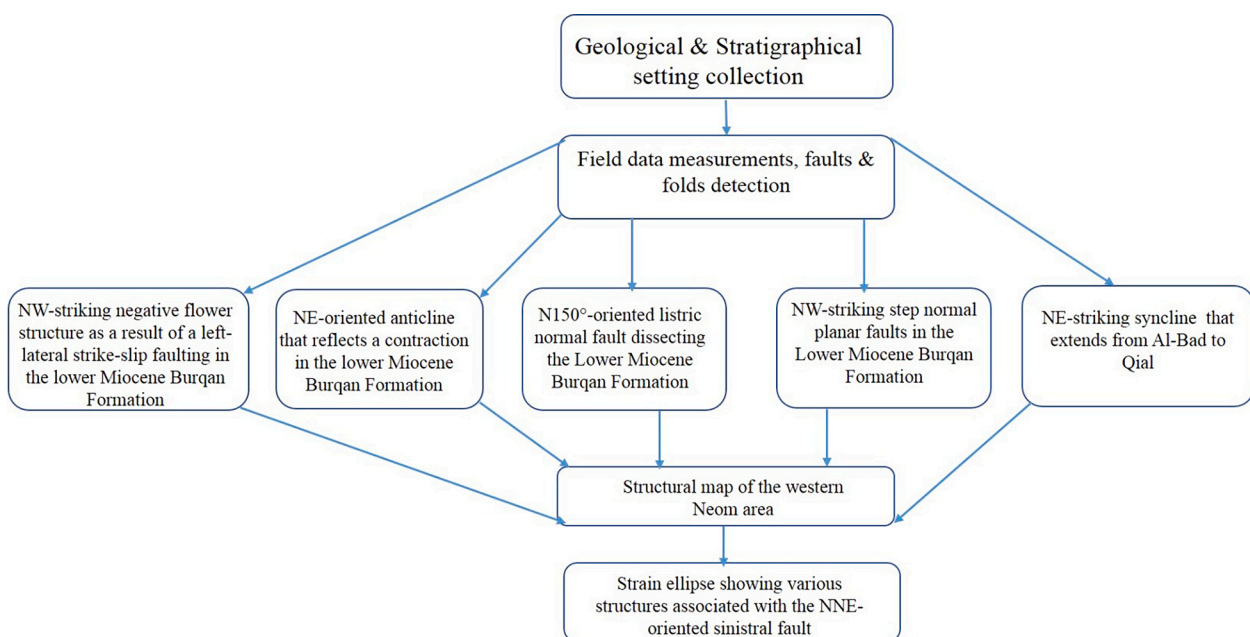


**Figure 2.** Flow chart showing the approach of the present study.

divergent Red Sea to the Zagros continental collision area via the NE-oriented sinistral East Anatolian Fault System in Turkey (Garfunkel 1981; Le Beon et al. 2008; Bosworth et al. 2017). This left-lateral fault system extends ~1000 km. It has accommodated ~105 km of left-lateral transform movement owing to the northward movement of the Arabia Plate relative to the Sinai subplate since the Early Miocene (~20 Ma; Freund et al. 1970).

The slip rate along the DSTF is 3-7.5 mm/year (Garfunkel 1981; Klinger et al. 2000; Niemi et al. 2001; Daëron et al. 2004; Marco and Agnon 2005; Reilinger et al. 2006; Ferry et al. 2007; Le Beon et al. 2008, 2010, 2012; Marco and Klinger 2014). The Dead Sea tectonic region was subjected to NNW–SSE compression and ENE–WSW extension related to the Middle Miocene–Recent sinistral movement along the Dead Sea Transform and the rifting of the Red Sea (Diabat et al. 2004). A paleoseismological trench along the southern section of the DSTF revealed 12 historical surface-rupturing earthquakes during the last 8000 years (Lefevre et al. 2018). The Mw 7.3 earthquake in the Gulf of Aqaba in 1995 indicates recent strong seismotectonic activity along the entire DSTF (Klinger et al. 1999; Hofstetter 2003). The investigated area of the western Neom area is located at the southeastern part of the DSTF system and northern reaches of the Red Sea Rift (Fig. 1). It displays a sequence of Neogene–Recent sedimentary rocks resting nonconformably on Precambrian metamorphic and igneous rocks of the Arabian Shield.

The western Neom area provides a unique opportunity to study the complicated tectonic stresses influencing the area through different time sequences. Few studies have been conducted regarding some structural settings of the area (Elawadi et al., 2013; Fnais et al., 2016; Kahal, 2020; Kahal et al., 2021; Ali and Abdelrahman, 2022; Alzahrani et al., 2022; Aboud et al., 2023; Bashir and Alsalman, 2024). The study attempts to detect and interpret the diversity of deformational structures and their field relationships within the exposed Neogene sequence in western Neom City. The results of the present study are expected to provide necessary data for decision-makers during the construction of the Neom mega-project.

## 2. Methodology

The approach of the present study includes a review of the previous literature, selecting sites for field investigation, detailed field measurements, interpretation of the structural elements, generating a structural map, and suggesting strain ellipse (Fig. 2). We carried out two field trips to investigate the different geological structures displayed in the study area. In the first trip, we conducted a reconnaissance survey using geological maps of the region (Clark 1986; Hughes et al. 1999) and satellite images (Google Earth) to select the best sites for detailed study and measurements of structural elements. Fortunately, the occurrence of drainage patterns and roadcuts provides excellent exposure to investigate and take measurements of the fractures, faults, and folds. The location of each selected site was defined using a GPS device. During the second trip, the attitudes (strike and dip) of faults, fractures, and tilted beds were measured using the Brunton compass. Extensive and careful examination has been given to the deformed rocks, displacements of faults, and mutual relationships among the various structures. The field measurements provided essential data for constructing a structural map and proposing a strain ellipse of the western Neom area (Fig. 2).

## 3. Tectonic Setting

Neom City is located at the juxtaposition of the Red Sea Rift and the Dead Sea Transform Fault (DSTF). The Red Sea Rift was initiated during the Late-Oligocene–Early-Miocene when the Arabian Shield separated from the Nubian Shield (Cochran and Martinez 1988; Ghebreab 1998). The average orientation of the Red Sea Rift from its southern end to Suez is N150° with an average ENE–WSW extension. The NNW-oriented basaltic dikes in southern Sinai and thick Miocene marine sediments reveal that the Gulf of Suez rift and the northern Red Sea were faulted in

the Early Miocene (Bartov et al., 1980). Strike-slip tectonic activity along the DSTF began in the Early Miocene (~20 Ma) (Freund et al. 1970). This type of tectonic activity yields a complex system of en-echelon arrays of fractures, faults, and folds developed within narrow, elongated zones. The DSTF is composed of numerous fault segments and accompanying transtensional and transpressional structures, such as pull-apart basins, pressure ridges, and fault scarps (Garfunkel 1981; Garfunkel and Freund 1981; Meghraoui et al. 2003; Daëron et al. 2004, 2007; Elias et al. 2007; Ferry et al. 2007; Marco 2007; Ben-Avraham et al. 2008; Abou Romieh et al. 2009; Le Beon et al. 2012). The geometrical and structural differences between the pure strike-slip Dead Sea pull-apart basin and transtensional Gulf of Aqaba complex series of pull-apart basins compare well analog model results.

The Dead Sea Transform system deformed the Neom Basin area in Saudi Arabia and the southern Sinai in Egypt (Bayer et al. 1988). Two phases of offset were identified. The first one, 62 km, occurred in the Miocene while the second, 45 km, occurred in the Pliocene to Recent. These movements connected a series of en-echelon faults and fractures to form a curved boundary between Neom and Sinai, creating the Gulf of Aqaba Rift and the triangular shape of the Neom (Bayer et al., 1988). Bosworth et al. (2005) proposed transferring the motion along the Gulf of Suez to the new Aqaba transform boundary in the Serravalian (Middle Miocene). The southern Gulf of Suez extends at only ~0.1 cm/year; nonetheless, the area is seismically active, whereas the south of the Gulf of Aqaba has not experienced any instrumentally recorded  $M \geq 5$  earthquakes (Bosworth et al. 2017). A major structural event, including folding and faulting, attributed to sinistral shearing, occurred in the Neom area during the Middle Miocene at 14–12 Ma (Bayer et al. 1988). This event coincided with Delaunay et al. (2023) proposed initiation of sea-floor spreading along the Red Sea trough.

## 4. Structural Architecture

### 4.1. Stratigraphic sequence

In the western Neom area, the Neogene sedimentary cover rests nonconformably on the Neoproterozoic metamorphic and crystalline rocks of the Midyan terrane at the northwestern Arabian Shield (Fig. 1). The oldest exposed Neogene sedimentary rocks belong to the Oligo–Miocene and are assigned to the Tayran Group composed of the Al-Wajh, Yanbu, and Musayr Formations. The Al-Wajh Formation (Hughes and Filatoff 1995) comprises laterally extensive, poorly sorted conglomerates with subordinate sandstones, red siltstones, and paleosols. These deposits rest unconformably on the Neoproterozoic basement rocks. In the subsurface, Hughes and Filatoff (1995) Yanbu Formation consists of anhydrite and halite, overlaying the Al-Wajh siliciclastics and, in places, are interbedded with them. Isolated hypersaline ponds deposited evaporites of the Yanbu Formation. The siliciclastics of the Al-Wajh Formation reach a thickness of 600 m at certain subsurface localities (Johnson et al. 1995). Still, where exposed in the Neom area, Lower Miocene shallow marine carbonates overlay them (the Musayr Formation of Clark 1986). They are well displayed north of Al-Bad and conformably overlain by Lower Miocene carbonates at Wadi Al Hamd. The Lower Miocene Burqan Formation unconformably rests on the Tayran Group. It comprises a thick succession of deep-marine calcareous mudstones with thick sand interbeds. The Middle Miocene Jabal Kibrit Formation unconformably overlays the Burqan Formation (Hughes and Filatoff 1995). Hughes et al. (1999) proposed that localized basement highs during the deposition of the Burqan Formation and sites of non-deposition continued until late Early Miocene when the carbonates of the Wadi Waqb member (Jabal Kibrit Formation, Maqna Group) were deposited. The carbonates of this formation are rich in corals. The Middle Miocene Kial Formation of the Maqna Group, consisting of four members (Hughes and Filatoff 1995; Johnson et al. 1995), conformably overlies the Jabal Kibrit Formation. A thick succession of massive gypsum, anhydrite, and halite, known as the Mansiyah Formation, overlays

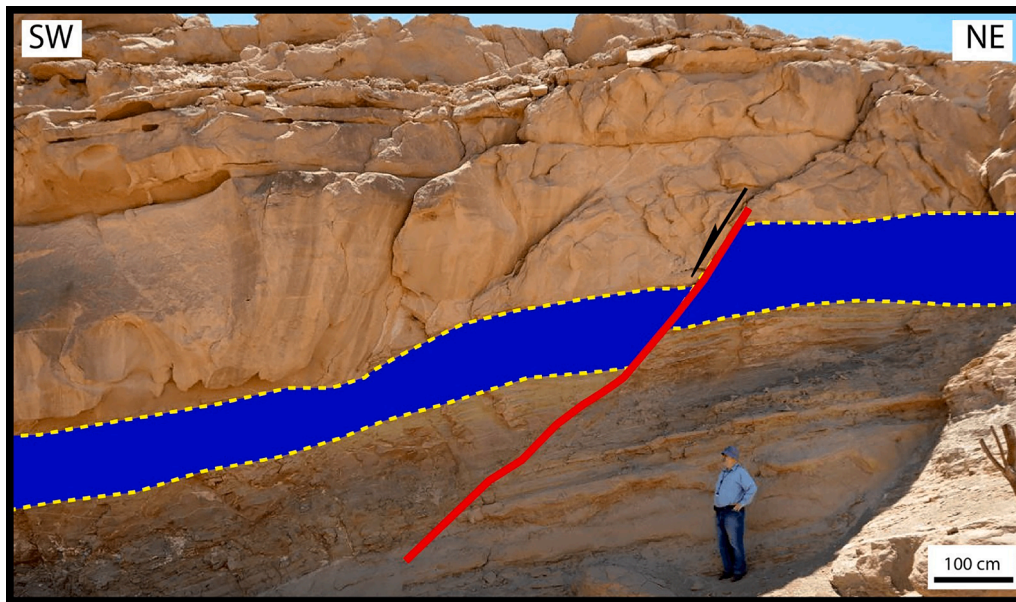


**Figure 3.** Field photograph showing N150°-oriented listric normal fault dissecting the Lower Miocene Burqan Formation, Maqna area. Figure 1 shows the location of this photograph.

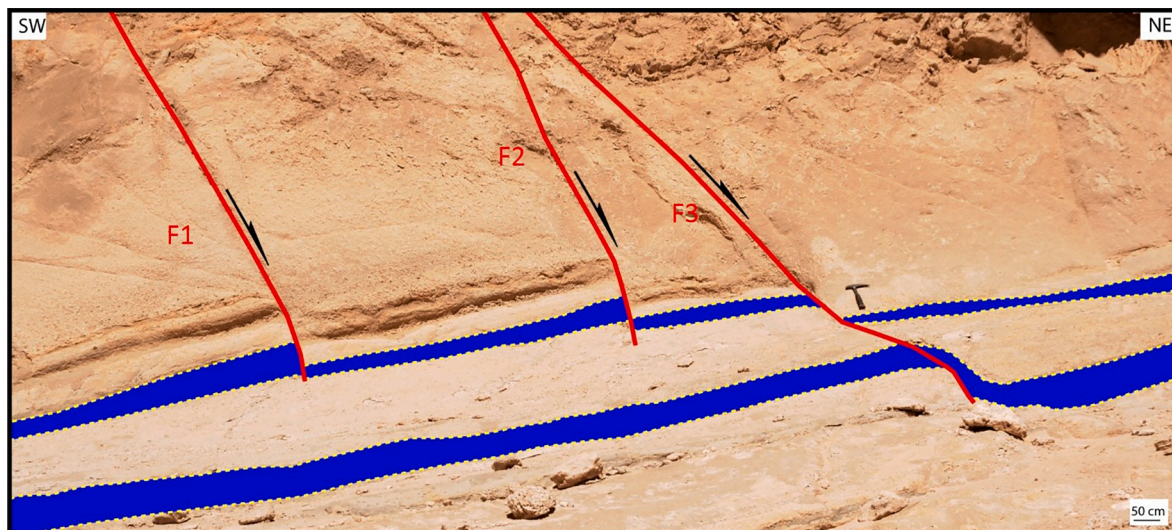


**Figure 4.** Field photograph showing NW-striking step normal planar faults (F1&F2) in the Lower Miocene Burqan Formation. Note Fault (F3), on the right side of the photo, has a listric surface.

the Kial Formation. The Middle to Upper Miocene Ghawwas Formation of Hughes and Filatoff (1995) conformably overlies this Middle to Upper Miocene Formation (Hughes et al. 1999). The Ghawwas Formation consists of a thick sequence of interbedded coarse- and fine-grained siliciclastics and thin anhydrite beds. The Plio-Quaternary sediments are mainly represented by raised beaches and wadi deposits.

#### 4.2. Evaluation of Structural Elements

##### 4.2.1. Red Sea Rift Extensional Structures

The NNW-oriented Red Sea continental rifting was initiated in the Late-Oligocene–Early-Miocene with normal faulting, extension, and subsidence accompanied by episodic movements of the Arabian plate away from Africa (Cochran and Martinez 1988; Ghebreab 1998). The Red Sea Rift is perpendicular to ENE–WSW-oriented extensional stresses generated by the convergence of the northeastern Africa–Arabia and Eurasian plates (Davison et al. 1994).

The coastal margins of the Gulf of Aqaba display N150° (NNW-oriented) en echelon right-stepping extensional faults that were linked to form a significant zigzag pattern. These NNW-oriented normal faults form significant fault scarps along most of the boundary between the Proterozoic basement rocks and the Neogene sedimentary cover in the Neom area (Fig. 1). During the initiation of the Red Sea Rift in the Oligo-Miocene, the Neom area was in the northern reaches of the rift when the left-lateral motion (~105 km) along the Dead Sea Transform was restored. This initial rifting stage was characterized by normal faulting, creating several NNW-oriented fault blocks. Moreover, NNW-oriented linear narrow reversed magnetic anomalies, extending parallel to the Red Sea Rift for kilometers in the Neom area, are interpreted as dikes intruded through syn-rift faults (Fnais et al. 2016). Although faults in the study area are mainly listric, planar fault planes exist. Near the Maqna area, Lower Miocene deposits are dissected by N150°-oriented listric normal faults (Fig. 3). These listric faults reflect the development of a half-graben pattern as individual fault blocks are antithetically tilted to

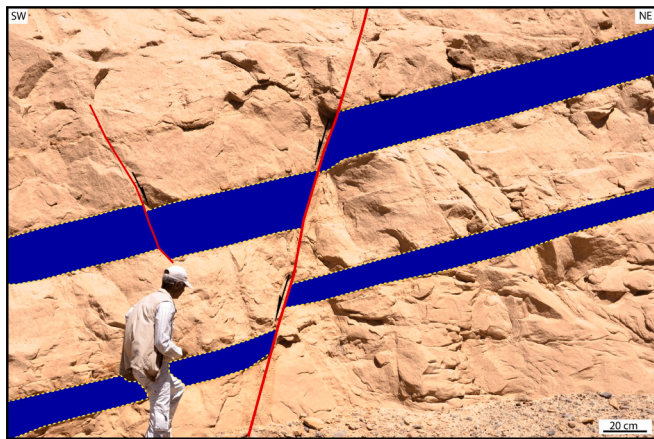


**Figure 5.** Field photograph showing NW-striking fault in the Lower Miocene Burqan Formation, located in the northern reaches of the study area.

the northeast. Field investigations revealed N50°–N60°-oriented oblique faults dissecting the NNW-oriented faults. These cross faults seem to have been activated during the extension of the Red Sea Rift. **Figure 4** shows NW-striking planar faults in the Lower Miocene Burqan Formation, located in the northern reaches of the study area, while **Figure 5** illustrates NW-striking step normal planar faults (F1&F2) in the Lower Miocene Burqan Formation. Note Fault (F3), on the right side of the

photo, has a listric surface.

#### 4.2.2. Dead Sea Transform Wrench Structures

Extensive irregular strike-slip faulting developed transtensive structures in western Neom. Transtension (divergent strike-slip) combines strike-slip displacement and extension, where the strike-slip fault might show a change in the strike direction or bend. The extension component causes normal faulting and subsidence. Transtension forms a significant deformation feature called a negative flower structure or a tulip structure (Naylor et al. 1986). We generated a structural map to show the nature and spatial distribution of the different structural elements at the Western Neom area (Fig. 6). The study area displays several subsidiary structures tectonically associated with strike-slip faults (Figs. 6 and 7). These secondary fractures are classified based on their orientation and sense of slip relative to the overall NNE-oriented strike-slip zone trend. One set is a synthetic NNW-oriented sinistral strike-slip fault (R shear), making a low angle (10°–15°) with the overall imposed shear zone and showing the same sense of slip. Another set of NNE-oriented fractures, known as P-shear fractures (P-shears), develops after establishing R-fractures, and their development relates to temporal variations in the local stress field along the shear zone as offset accumulates. The faults of this set are roughly parallel to the rift and diverge by approximately –10° from the Dead Sea Rift. The third set of shear fractures (R' shears) is antithetic WNW-oriented dextral strike-slip faults, making a high angle (70°–80°) to the zone (Fossen 2010).

Oblique faults with strike-slip and normal displacements occur

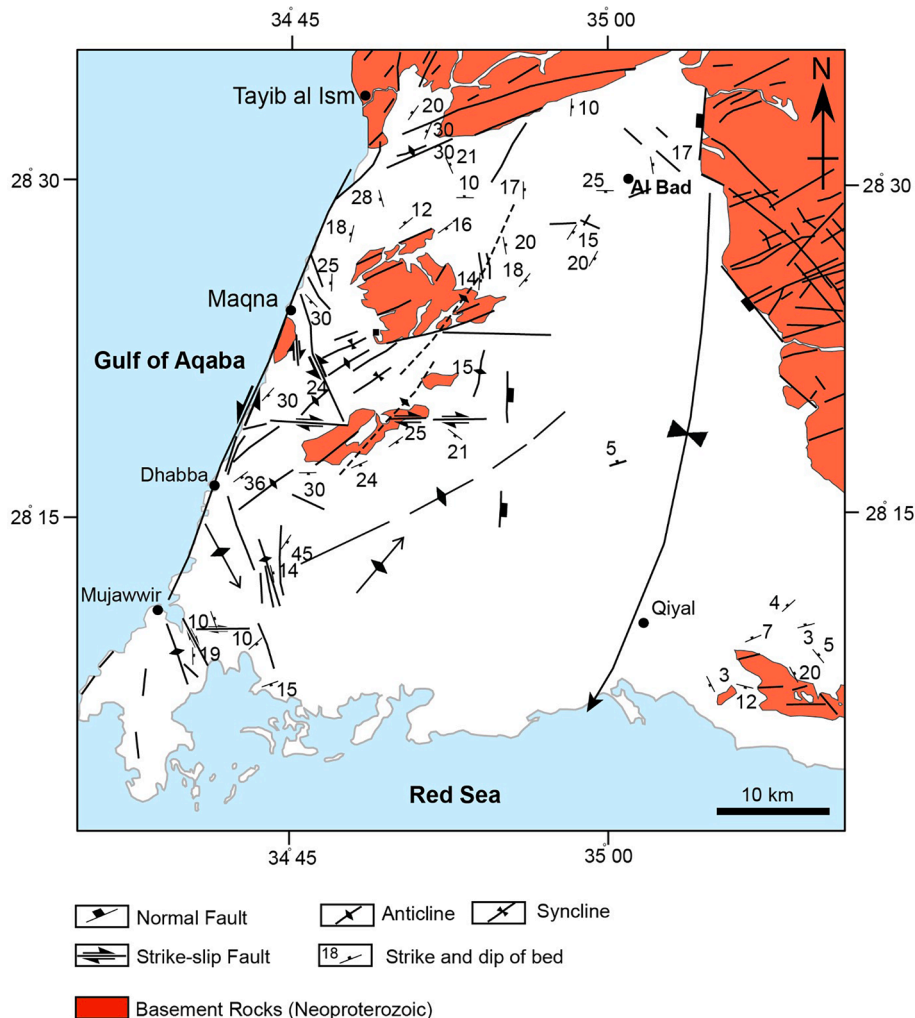


**Figure 6.** Structural map of the western Neom area. The syncline fold that extends from Al-Bad to Qial is from Bayer et al. (1988).

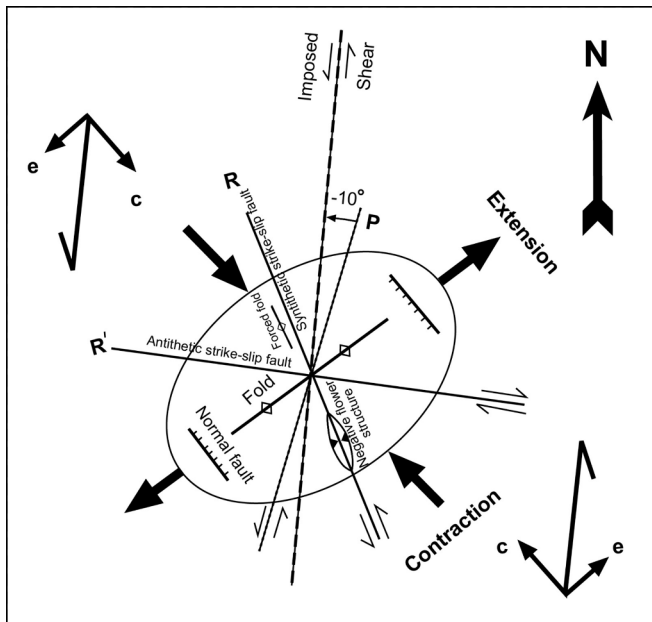


**Figure 7.** Strain ellipse showing various structures associated with the NNE-oriented sinistral fault. R and R' represent the Riedel system, P is P-shear, c is the contractional vector, and e is the extensional vector.

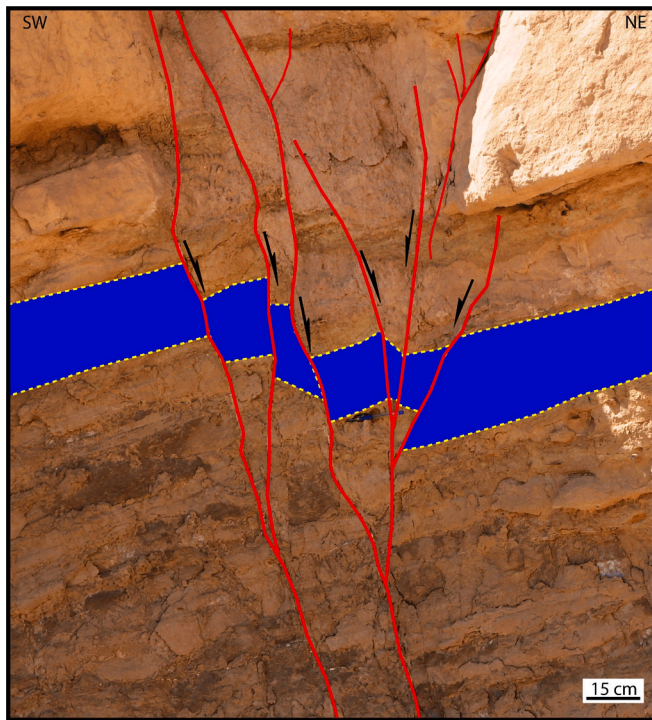


**Figure 8.** Field photo showing NW-striking negative flower structure as a result of a left-lateral strike-slip faulting in the lower Miocene Burqan Formation, south of Maqna area. The dip-slip movement of the faults reflects extension by normal faults. The faults are filled with gypsum. The blue pen in the middle of the photo is for scale.

within a few kilometers of the coast of the Gulf of Aqaba. In western Neom, the fault planes are wavy and branch upwards, characteristic features of a negative flower structure (Fig. 8). As the negative flower structure evolves, connecting faults die out individually, and new faults form. Each fault connects with the master strike-slip fault, assuring a linkage and kinematic organization. Field investigations of the slicklines

indicate sinistral movement along the NNW-oriented master strike-slip fault and normal dip-slip movements along the branching faults of the negative flower structure. This master fault represents the synthetic NNW-oriented sinistral strike-slip fault set (R shear) (Fig. 7).

Folds are associated with sinistral strike-slip faults in the western Neom (Fig. 1) and characterized by their en-echelon arrangement. The folds are formed either in sets or as isolated anticlines and synclines. A set of NE-oriented left-handed en echelon-arranged folds occurred in the Middle Miocene deposits of the study area (Fig. 1). South of Magna, we observed NW-striking negative flower structure that can be attributed to a left-lateral strike-slip faulting in the lower Miocene Burqan Formation. The dip-slip movement along the hanging walls of the faults reflects extension by normal faults (Fig. 8). It is noted that the faults are filled with gypsum. In addition, an NE-oriented anticline reflects a contraction in the lower Miocene Burqan Formation, south of the Maqna area. Both limbs of the fold are dissected by NE-striking reverse faults resembling a probable positive flower structure (Fig. 9).

### 5. Discussion, Conclusions, and Recommendations

The western Neom area exhibits a diverse assemblage of structural elements. It displays NNW-oriented normal faults running parallel to the Red Sea Rift, reflecting the influence of the rift-related extensional tectonics of the Red Sea on the study area. The kinematics of the Red Sea regime changed in the Late Miocene from rifting with an ENE–WSW extension to a left-lateral shear along the NNE-oriented sinistral transform fault system along the Gulf of Aqaba and the Dead Sea. From GPS datasets, Arabia would move NNE relative to Africa/Nubia at ~0.68 cm/yr (Reilinger et al. 2006). In western Neom, the sinistral motion onset along the DSTF postdates the Lower Miocene Burqan Formation deposition. However, the sinistral strike-slip regime of the west of Neom area consists of extensional structures, including normal faults, contractional structures, such as folds, and deformation reflecting a horizontal shear on nearly vertical planes. Fortunately, the concept of wrench tectonics can explain the occurrence of these structures (Moody and Hill, 1956). The variety and complexity of these structural elements display three main characteristics (Naylor et al. 1986): (1) lateral offsets of basement-involved strike-slip faults, creating extensional or contractional structures; (2) an echelon arrangement of faults and folds; and (3) complications owing to reverse or normal dip-slip components on deep-seated faults. A set of NE-oriented left-handed en echelon-arranged folds deformed the Middle Miocene deposits. Besides, negative flower structures and N07°W-oriented overturned anticline developed along the synthetic NNW-oriented sinistral strike-slip fault set (R shear) in the southwestern part of the Neom area. The overturned anticline developed as a fault-propagation fold. Variable fault orientations (NW–SE-oriented normal faults, WNW–ESE and ENE–WSW-oriented oblique-slip faults, and NNE–SSW and NW–SE trending strike-slip faults) dissect the rocks in the Neom area. These fault trends might reflect rejuvenated basement faults because they are expected within the Precambrian basement rocks. The suggested strain ellipse shows that this variety of structures is associated with the NNE-oriented sinistral Dead Sea Fault. Therefore, the complexity and variety of the structural architecture in western Neom indicate that its evolution has passed through two tectonic scenarios depending on the effect of prevailing stress. Extensional stress that led to the Red Sea–Gulf of Suez rifting governed the first scenario, whereas shear stress that resulted in the Dead Sea wrench structures controlled the second one.

Since the study area hosts the developmental urban Neom city, we highly recommend the decision-makers consider the nature and spatial distribution of its geological structures during the design and construction of such a vital mega-project. Furthermore, a detailed geotechnical investigation regarding the attitudes of fracture planes at each site is mandatory before embarking upon the construction. The orientation of fracture surfaces must be understood since fractures are zones of weakness in rocks. Since each site has its structural peculiarity,

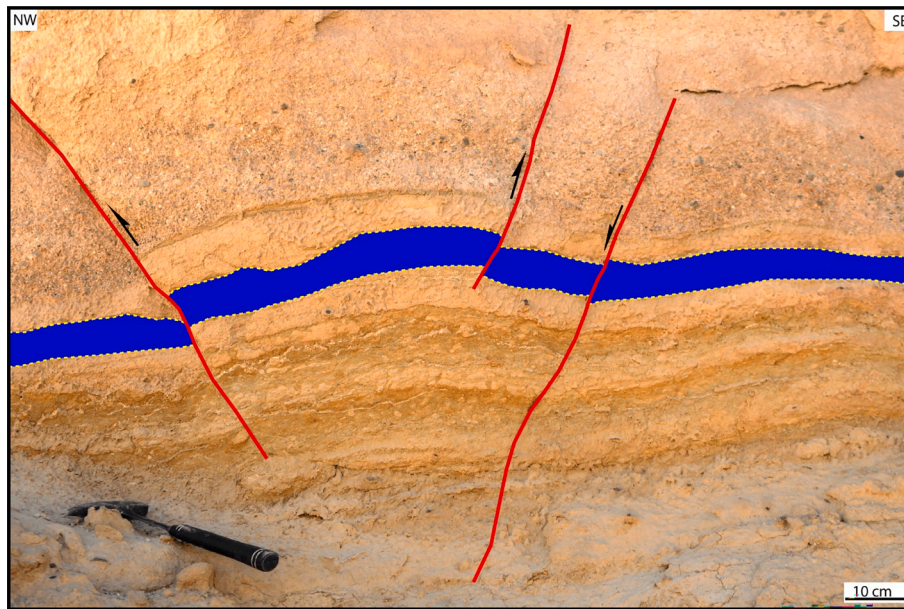


**Figure 9.** Field photograph showing a NE-oriented anticline that reflects a contraction in the lower Miocene Burqa Formation, south of Maqna area. A NE-striking reverse fault dissects the northwestern limb of the fold.

the critical issue is that after excavating the foundation and abutment, an accurate picture of fractures will emerge to be considered in the final design.

#### CRediT authorship contribution statement

**Ali Y. Kahal:** Writing – review & editing, Writing – original draft, Funding acquisition, Formal analysis, Data curation, Conceptualization.  
**Essam Abd El-Motaal:** Writing – review & editing, Writing – original draft, Validation, Methodology, Conceptualization.

#### Declaration of competing interest

The authors declare that they have no known competing financial interests or personal relationships that could have appeared to influence the work reported in this paper.

#### Acknowledgments

The authors sincerely thank the Researchers Supporting Project number (RSPD2024R546) at King Saud University in Riyadh, Saudi Arabia, for funding this research article. We also thank the editor-in-chief and reviewers for their detailed reviews and constructive comments, significantly improving the manuscript.

#### Appendix A. Supplementary data

Supplementary data to this article can be found online at <https://doi.org/10.1016/j.jksus.2024.103532>.

#### References

- Abou, R., Westaway, R., Daoud, M., Radwan, Y., Yassminh, R., Khalil, A., Al-Ashkar, A., Loughlin, S., Arrell, K., Bridgland, D., 2009. Active crustal shortening in NE Syria revealed by deformed terraces of the River Euphrates. *Terra Nova* 21, 427–437. <https://doi.org/10.1111/j.1365-3121.2009.00896.x>.
- Aboud, E., Alqahtani, F., Abdulfarrag, M., Abraham, E., El-Masry, N., Osman, H., 2023. Geothermal imaging of the Saudi cross-border city of NEOM deduced from magnetic data. *Sustainability* 15, 4549.
- Ali, S.M., Abdelrahman, K., 2022. Earthquake occurrences of the major tectonic terranes for the Arabian shield and their seismic hazard implications. *Front. Earth Sci.* 10, 851737. <https://doi.org/10.3389/feart.2022.851737>.

- Alzahrani H., Abdelrahman K., Qaysi S., Baras M. (2022) Seismicity of the Neom megaproject area, Northwestern Saudi Arabia. *Journal of King Saud University – Science* 34 (2022) 101659. [10.1016/j.jksus.2021.101659](https://doi.org/10.1016/j.jksus.2021.101659).
- Bashir, B., Alsaman, A., 2024. (2024) Morpho-hydrological analysis and preliminary flash flood hazard mapping of Neom city, northwestern Saudi Arabia. Using Geospatial Techniques. *Sustainability* 16, 23. <https://doi.org/10.3390/su16010023>.
- Ben-Avraham, Z., Garfunkel, Z., Lazar, M., 2008. Geology and evolution of the southern Dead Sea fault with emphasis on subsurface structure. *Ann Rev Earth Planet Sci* 36, 357–387.
- Bosworth, W., Montagna, P., Pons-Branchu, E., Rasul, N., Taviani, M., 2017. Seismic Hazards implications of uplifted Pleistocene coral terraces in the Gulf of Aqaba. *Scientific Reports* 7, 1–13. <https://doi.org/10.1038/s41598-017-00074-2>.
- Clark MD (1986) Explanatory notes to the geologic map of the Al Bad' quadrangle, sheet 28A, Kingdom of Saudi Arabia: Saudi Arabian Deputy Ministry for Mineral Resources Geoscience Map Series GM-81A, C, Scale 1:250,000, with text, p 46.
- Cochran, J., Martinez, F., 1988. Structure and tectonics of the Northern Red Sea: catching a continental margin between rifting and drifting. *Tectonophysics* 150, 1–32.
- Daëron, M., Klinger, Y., Tapponnier, P., Elias, A., Jacques, E., Surssock, A., 2007. 12,000-year-long record of 10 to 13 paleoearthquakes on the Yammouneh Fault, Levant Fault system, Lebanon. *Bull Seismol Soc Am* 97, 749–771.
- Davison, I., Al-Kadasi, M., Al-Khribash, S., Al-Subbary, A., Baker, J., Blakey, S., Bosence, D., Dart, C., Heaton, R., McClay, K., Menzies, M., Nichols, G., Owen, L., Yelland, A., 1994. Geological evolution of the southeastern Red Sea Rift margin, Republic of Yemen. *Geol Soc Am B* 106, 1474–1493. [https://doi.org/10.1130/0016-7606\(1994\)106<1474:geotrs>2.3.co;2](https://doi.org/10.1130/0016-7606(1994)106<1474:geotrs>2.3.co;2).
- Delaunay, A., Baby, G., Alafifi, A., Fedorik, J., Dymont, J., Tapponnier, P., 2023. Structure and morphology of the Red Sea. From the Mid-Ocean Ridge to the Ocean-Continent Boundary. *SSRN Electronic Journal* 849 10.2139/ssrn.4246850.
- Diabat, A., Atallah, M., Salih, M., 2004. Paleostress analysis of the Cretaceous rocks in the eastern margin of the Dead Sea transform. *Jordan. J. Afr. Earth. Sci.* 38, 449–460. <https://doi.org/10.1016/j.jafrearsci.2004.04.002>.
- Elawadi, E., Haider, Z., Awani, B., Mogren, S., Laboun, A., Ghrefat, H., 2013. Zumlot T (2013) Structural interpretation of the Ifal Basin in north-western Saudi Arabia from aeromagnetic data: hydrogeological and environmental implications. *Explor Geophys* 44, 251–263. <https://doi.org/10.1071/EG12069>.
- Elias, A., Tapponnier, P., Singh, S., King, G., Briaies, A., Daëron, M., Carton, H., Surssock, A., Jacques, E., Jomaa, R., Klinger, Y., 2007. Active thrusting offshore Mount Lebanon: source of the tsunamigenic A.D. 551 Beirut-Tripoli earthquake. *Geology* 35, 755–758.
- Ferry, M., Meghraoui, M., Abou-Karaki, N., Al-Taj, M., Amoush, H., Al-Dhaisat, S., Barjous, M., 2007. A 48-kyr-long slip rate history for the Jordan Valley segment of the Dead Sea Fault. *Earth Planet Sci Lett* 260, 394–406.
- Fnaies, M., Ibrahim, E., Abd El-Motaal, E., Abdelrahman, K., Al-Henedi, A., Al-Kahtany, K., 2016. Structural development of northwest Saudi Arabia using aeromagnetic and seismological data. *J Earth Sci* 27, 998–1007. <https://doi.org/10.1007/S12583-016-0904-0>.
- Fossen, H., 2010. *Structural geology*. Cambridge University Press, Cambridge.
- Ghebreab, W., 1998. Tectonics of the Red Sea region reassessed. *Earth Sci Rev* 45, 1–44.
- Hofstetter, A., 2003. Seismic observations of the 22/11/1995 Gulf of Aqaba earthquake sequence. *Tectonophysics* 369, 21–36.

- Hughes G, Filatoff J (1995) New biostratigraphic constraints on Saudi Arabian Red Sea pre- and syn-rift sequences. In Al-Husseini ML (ed) Middle East Petroleum Geosciences, Geo'94, Vol 2. Gulf PetroLink, Bahrain, 517–528.
- Hughes, G.W., Perincek, D., Grainger, D.J., Abu-Bshait, A., Jarad, A.M., 1999. Lithostratigraphy and depositional history of part of the Midyan region, Northwest Saudi Arabia. *GeoArabia* 4, 503–542.
- Johnson RS, Rodgers D, Savage GR (1995) Red Sea Exploration Program, Saudi Arabia Coastal Plain. Saudi Aramco Miscellaneous Report 1029.
- Kahal, A.Y., 2020. Geological assessment of the Neom mega-project area, northwestern Saudi Arabia: an integrated approach. *Arab. J. Geosci* 13, 345. <https://doi.org/10.1007/s12517-020-05345-3>.
- Kahal, A.Y., Abdelrahman, K., Alfaihi, H.J., Yahya, M.A., 2021. Landslide hazard assessment of the Neom promising city, northwestern Saudi Arabia: An integrated approach. *J. King Saud Univ. Sci.* 33 (2), 101279. <https://doi.org/10.1016/j.jksus.2020.101279>.
- Klinger, Y., Avouac, J., Abou-Karaki, N., Dorbath, L., Bourles, D., Reyes, J., 2000. Slip rate on the Dead Sea Transform fault in the northern Araba Valley (Jordan). *Geophys J Int* 142, 755–768. <https://doi.org/10.1046/j.1365-246X.2000.00166.x>.
- Le Béon, M., Klinger, Y., Mériaux, A.-S., Al-Qaryouti, M., Finkel, R.C., Mayyas, O., Tapponnier, P., 2012. Quaternary morphotectonic mapping of the Wadi Araba and implications for the tectonic activity of the southern Dead Sea fault. *Tectonics* 31, 1–25. <https://doi.org/10.1029/2012TC003112>.
- Lefevre, M., Klinger, Y., Al-Qaryouti, M., Le Béon, M., Moumani, K., 2018. Slip deficit and temporal clustering along the Dead Sea fault from paleoseismological investigations. *Sci Rep* 8, 4511. <https://doi.org/10.1038/s41598-018-22627-9>.
- Marco, S., 2007. Temporal variation in the geometry of a strike-slip fault zone: examples from the Dead Sea Transform. *Tectonophysics* 445, 186–199.
- Marco, S., Agnon, A., 2005. High-resolution stratigraphy reveals repeated earthquake faulting in the Masada Fault Zone. *Dead Sea Transform Tectonophysics* 408, 101–112.
- Meghraoui, M., Gomez, F., Sbeinati, R., derWoerd, J., Mouty, M., Darkal, A., Radwan, Y., Layyous, I., Najjar, H., Darawcheh, R., Hijazi, F., Al-Ghazzi, R., Barazangi, M., 2003. Evidence for 830 years of seismic quiescence from palaeoseismology, archaeoseismology and historical seismicity along the Dead Sea fault in Syria. *Earth Planet Sci Lett* 210, 35–52.
- Naylor, M., Mandl, G., Sijpesteijn, C., 1986. Fault geometries in basement induced wrench faulting under different initial stress states. *J Struct Geol* 8, 737–752.
- Niemi, T., Zhang, H., Atallah, M., Harrison, J., 2001. Late Pleistocene and Holocene slip rate of the Northern Wadi Araba fault, Dead Sea Transform, Jordan. *J Seismol* 5, 449–474. <https://doi.org/10.1023/A:1011487912054>.
- Ribot, M., Lefèvre, M., Klinger, Y., Pons-Branchu, E., Dapoigny, A., Jónsson, S., 2024. Vertical deformation along a strike-slip plate boundary: The uplifted marine terraces of the Gulf of Aqaba and Tiran Island, at the southern end of the Dead Sea Fault. *Tectonics* 43. <https://doi.org/10.1029/2023TC007977>.